Bibliography

1. Anzer U., Heinzel P., 1999, A&A 349, 974
2. Anzer U., Heinzel P., 2000, A&A 358, L75
3. Athay R.G., Dere K.P., 1989, ApJ 346, 514
4. Athay R.G., Holzer T.E., 1982, ApJ 225, 743
5. Auer L.H., Paletou F., 1994, A&A 285, 675
6. Bates D.R., Kingston A.E., McWhirter R.W.P., 1962, Proc. Royal Society London, 267A, 297
7. Beckers J.M., 1972, Ann. Rev. Astron. Astrophys. 10, 73
8. Behringer K.H., 1997, Max Plank Institut fuer Plasmaphysik report IPP 10/5
9. Bhatia A.K., Kastner S.O., 1997, J. Quant. Spectrosc. Radiat. Transfer 58, 347
10. Bhatia A.K., Kastner S.O., 1999, ApJ 516, 482
11. Brekke P., Hassler D.M., Wilhelm K., 1997, Solar Phys. 175, 349
12. Brooks D.H., 1997, Ph.D. Thesis, Univ. of Strathclyde
13. Brooks D.H., Fischbacher G.A., Fludra A., 2000, A&A 357, 697
14. Brooks D.H., Summers H.P., Harrison R.A. et al., 1998, Astrophys Space Sci. 261, 91

15. Budnik F., Schröder K.-P., Wilhelm K. et al., 1998, A&A 334, L77

16. Burgess A., Summers H.P., 1969, ApJ 157, 1007

17. Carlsson M., 1986, Technical Report 33, Uppsala Astronomical Observatory

18. Carlsson M., 1997, Proceedings of a Summer School Held in Orsay, France, 1-13 September 1997

19. Chae J., Yun H.S., Poland, A.I., 1998, ApJS, 114,151

20. Code A.D., Whitney B.A., 1995, ApJ 441, 400

21. Craig I.J.D., Brown J.C., 1973, Solar Phys. 49, 239

22. David C., Gabriel A.H., Bely-Debau, 1997, Proceedings of the Fifth SOHO Workshop, Oslo, Norway, 17-30 June, 1997

23. Domingo V., Fleck B., Poland A.I., 1995, Solar Phys. 162, 1

24. Doschek G.A., Vanhoosier M.B., Bartoe J.-D.R. et al., 1976, ApJS 31, 417

25. Doyle J.G., McWhirter R.W.P., 1980, MNRAS 193, 947

26. Doyle J.G., Teriaca L., Banerjee D., 2000, A&A 356, 335

27. Fledman U., Cohen L., Doschek G.A., 1982, ApJ 255, 325

28. Feldman U., Lamming J.M., 1994, ApJ 434, 370

29. Feutrier P., 1964, C.R. Acad. Sci. Paris, 258, 3189

30. Fontenla J.M, Rovira M., Vial J.-C. et al., 1996, ApJ 466, 496

31. Gontikakis C., Vial J.-C., Gouttebroze P., 1997, A&A 325, 803

32. Gouttebroze P., Heinzel P., Vial J.-C., 1993, A&AS 99, 513

33. Gouttebroze P., Vial J.-C., Tsiropoula G., 1986, A&A, 154, 154

34. Heasley J.N., Mihalas D., 1976, ApJ 210, 827

35. Heinzel P., 1995, A&A 299, 563

36. Heinzel P., Brommier V., Vial J.-C., 1996, Solar Phys. 164, 211

37. Heinzel P., Gouttebroze P., Vial J.-C., 1987, A&A 183, 351

38. Henze W., Engvold O., 1992, Solar Phys. 141, 51

39. Holstein T., 1947, Phys. Rev. 72, 1212

40. Hubeny I., Lites B.W., 1995, ApJ 455, 376

41. Hummer D.G., Rybicki G.B., 1982, ApJ 263, 925

42. Irons F.E., 1979, J. Quant. Spectrosc. Radiat. Transfer 22, 1

43. Ishizawa T., 1971, Publ. Astron. Soc. Japan 23, 75

44. Jordan C., 1967, Solar Phys. 2, 441

45. Kastner S.O., 1999, Physica Scripta 60, 381

46. Kastner S.O., 1981, J. Quant. Spectrosc. Radiat. Transfer 26, No. 4, 377

47. Kastner S.O., Bhatia A.K., 1989, ApJS 71, 665

48. Kastner S.O., Bhatia A.K., 1992, ApJ 401, 416

49. Kastner S.O., Kastner R.E., 1990, J. Quant. Spectrosc. Radiat. Transfer 44, No. 2, 275

50. Keenan R.P., Kingston A.B., 1986, MNRAS 220, 493

51. Lanzafame A.C., 1994, A&A 287, 792

52. Lemaire P., 1998, private communication

53. Loch S.D., 2001, Ph.D. Thesis, Univ. of Strathclyde

54. Lorrain P., Koutchmy S., 1993, A&A 269, 518

55. Lorrain P., Koutchmy S., 1996, Solar Physics 165, 115

56. Mariska J.T., Feldman U., Doschek G.A., 1978, ApJ 226, 698

57. McWhirter R.W.P., 1965, In: Huddlestone R.H., Leonard D.H. (eds), Plasma Diagnostic Techniques, Accademic Press, Inc.

58. McWhirter R.W.P., Summers H.P., 1984, In: Masset H.S.W., McDaniel E.W., Bederson B. (eds), Applied Atomic Collision Physics, Accademic Press, Inc.

59. Mein N., Mein P., Heinzel et al., 1996, A&A 309, 275

60. Mihalas D., 1978, Stellar Atmospheres (2nd ed.), W.H. Freeman & Co., San Fransisco

61. Mitchell A.C.G., Zemansky M.W., 1961, Resonance radiation and excited atoms, Cambridge University Press

62. Olson G.L., Auer L.H., Buchler J.R., 1986, J. Quant. Sectrosc. Radiat. Transfer 35, 431

63. Orrall F.Q., Schmahl E.J., 1980, ApJ 240, 908

64. Paletou F., 1995, A&A 302, 587

65. Paletou F., 1996, A&A 311, 708

66. Paletou F., Vial J.-C., Auer L.H., 1993, A&A 274, 571

67. Papushev P.G., Salakhutdinov R.T., 1994, Space Science Rev. 70, 47

68. Phillips K.J.H., 1992, Guide to the Sun, Cambridge University Press

69. Poland A., Skumanich A., Athay R.G. et al., 1971, Solar Phys. 18,391

70. Roberts W.O., 1945, ApJ 101, 136

71. Rybicki G.B., Hummer D.G., 1991, A&A 245,171

72. Rybicki G.B., Hummer D.G., 1992, A&A 262, 209

73. Secchi P.A., 1877, Le Soleil, Vol. 2, Chap II, Paris, Gauthier-Villars

74. Spadaro D., Lanza A.F., Antiochos S.K., 1996, Ap.J. 462, 1011

75. Spitzer L., 1956, 'Physics of Fully Ionised Gases', Interscience, NY

76. Vernazza J.B., Avrett B.H., Loeser R., 1981, ApJS 45, 635

77. Wilhelm K., Curdt W., Marsch B. et al., 1995, Solar Phys. 162, 189

78. Withbroe G.L., 1983, ApJ 267, 825

79. Withbroe G.L., Mariska J.T., 1976, Solar Phys. 48, 21

80. Wood K., Raymond J., 2000, ApJ 540, 563

81. Zheng W., Davidsen A.F., Kriss G.A., 1998, ApJ 115, 391

Appendix A

The assumption of constant source function: results for the exponential density case

The absorption factor analysis described in sec. 3.4 applies to a stratified, plane parallel atmosphere and may be performed using any density distribution, $N_l(x)$. The absorption factors shown in figs 3.5 and 3.6 and the corresponding density distributions shown in figs 3.8 $\rightarrow$ 3.11 are shown here for an exponential density model (model 3). The agreement between $\Lambda(\tau_0, x)$ and $\mathcal{G}(\tau_0, x)$ is not greatest at layer centre but in between layer centre and the point of peak emission. Thereafter, however, the same conclusions follow as in chapter 3. The agreement between $\Lambda(\tau_0, x)$ and $\mathcal{G}(\tau_0, x)$ decreases toward the layer edges and with optical depth. The $\Lambda(\tau_0, x)$ versus x trends deviate from those of $\mathcal{G}(\tau_0, x)$ most markedly for lines that share an upper level with a line thicker than themselves. The density distributions do not display these indirect effects and are modified in a similar manner to those in the constant density case but with the point of most significant modification begin between layer centre and the point of peak emission. The corresponding limb-brightening curves are shown in figs 3.12b and 3.13b.

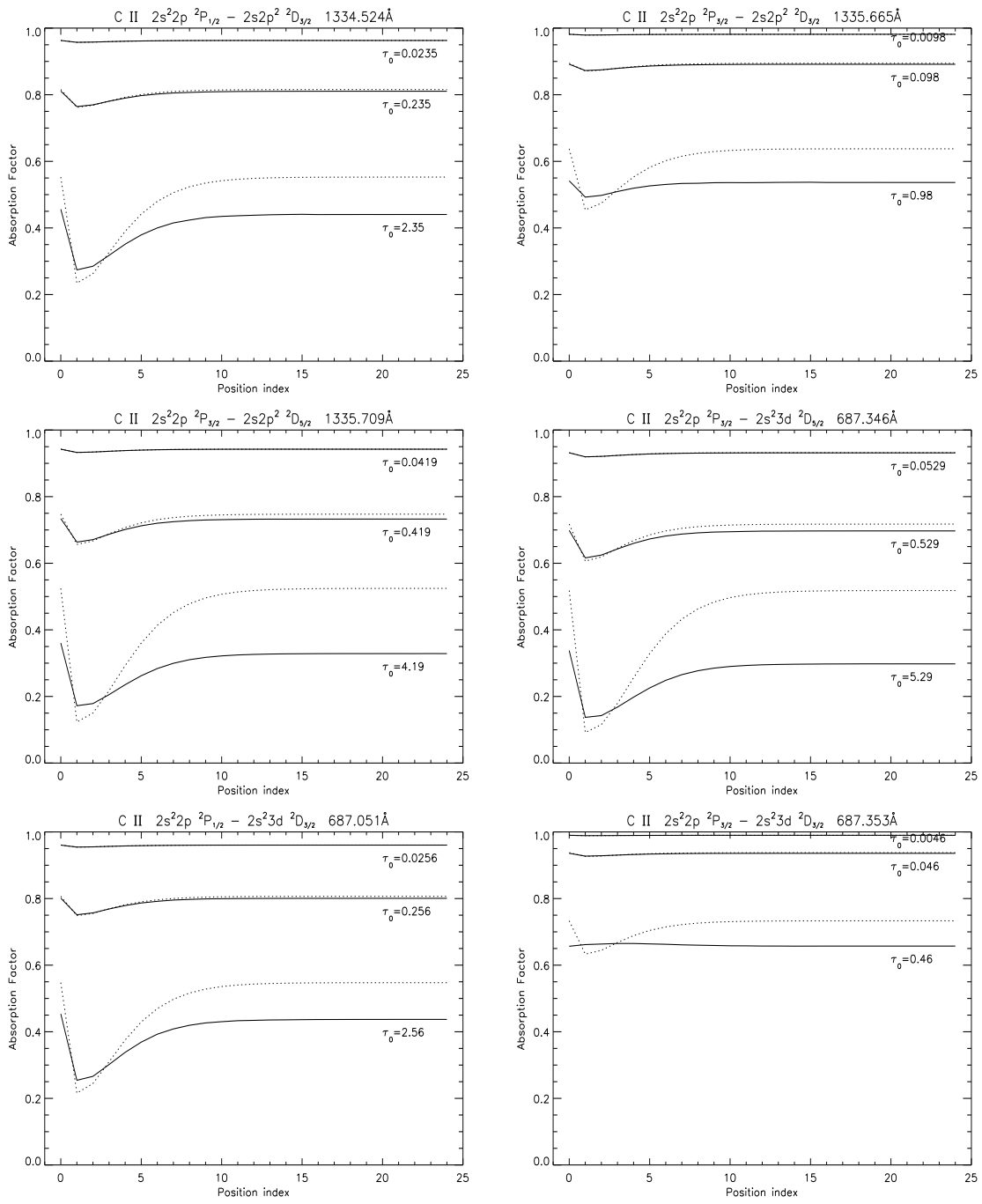

Figure A.1: Absorption factors versus position for selected lines of C II corresponding to three sets of optical depths. Absorption factors are calculated iteratively via eqs 3.15 and 2.8 in an exponential density model. The solid lines are $\Lambda(\tau_0, x)$ and the dotted lines are $\mathcal{G}\{\tau_0, x\}$. These plots are comparable with those in fig. 3.5

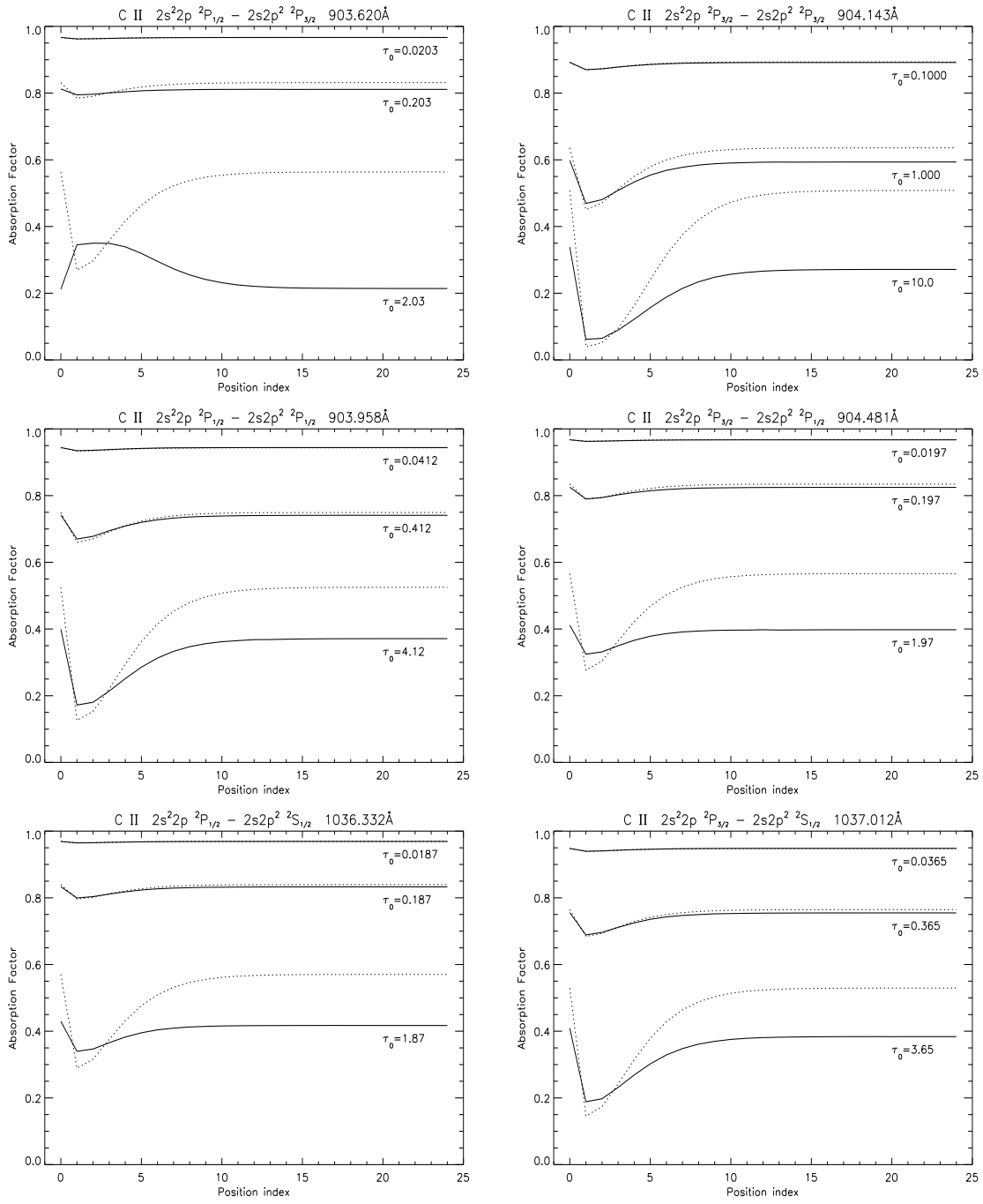

Figure A.2: Absorption factors versus position for selected lines of C II as in fig A.1. These plots are comparable with those in fig. 3.6.

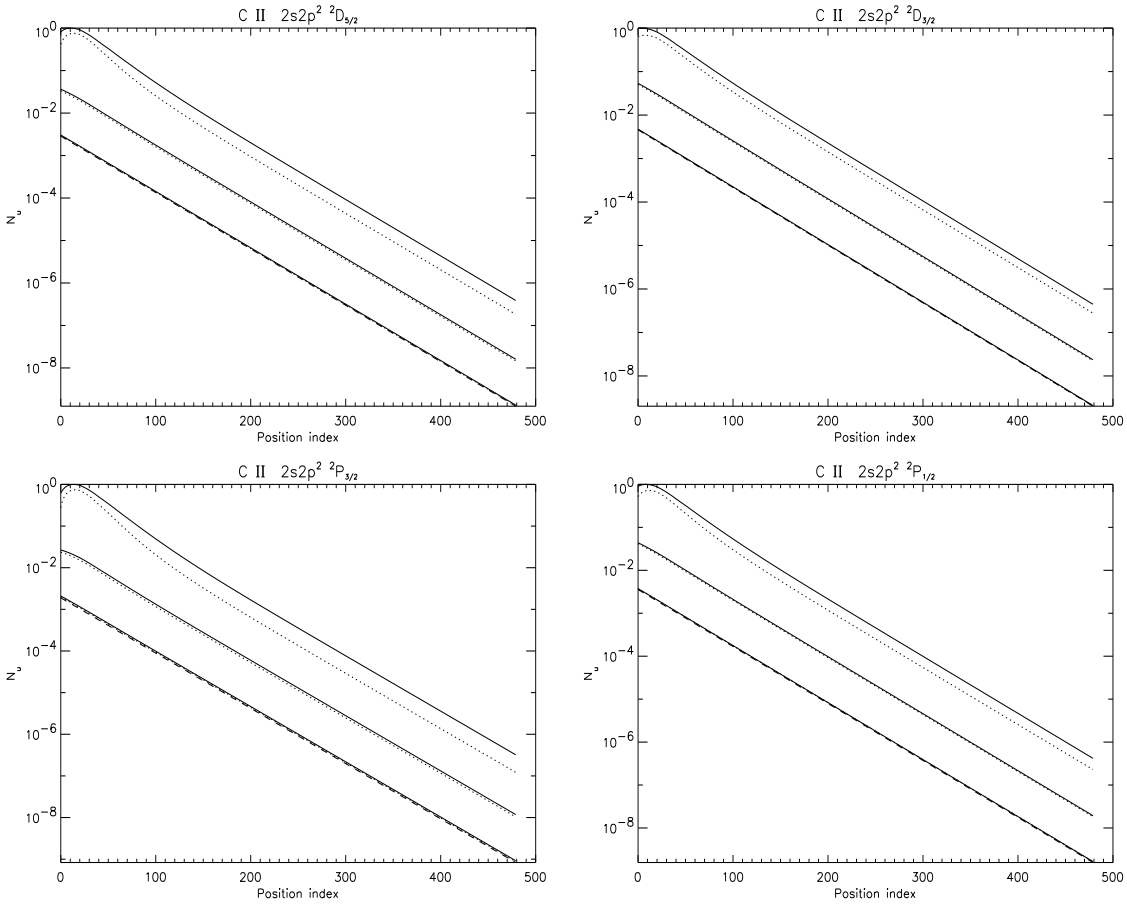

Figure A.3: Upper level population densities versus spatial position for selected levels of C II calculated in an exponential density model. The solid lines correspond to calculations based on $\Lambda(\tau_0, x)$ for the same three sets of optical depths as in figs A.1 and A.2. The dotted lines represent the $\mathcal{G}(\tau_0, x)$ based calculations. Values are not absolute but are scaled so that the maximum population density value is unity. These plots are comparable with those in fig. 3.8

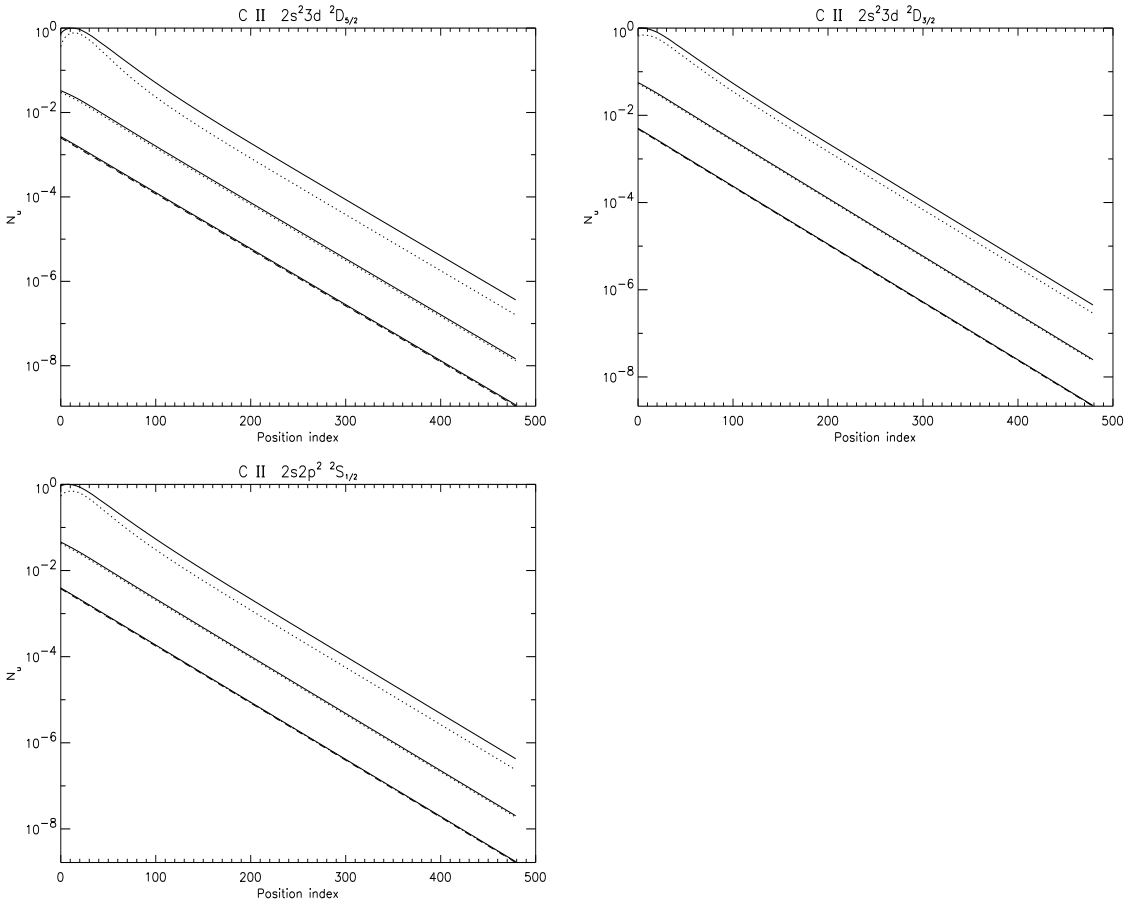

Figure A.4: Upper level population densities versus spatial position for selected lines of C II calculated in an exponential density model. The solid and dotted lines are as in fig. A.3. Values are not absolute but are scaled so that the maximum population density value is unity. These plots are comparable with those in fig. 3.9

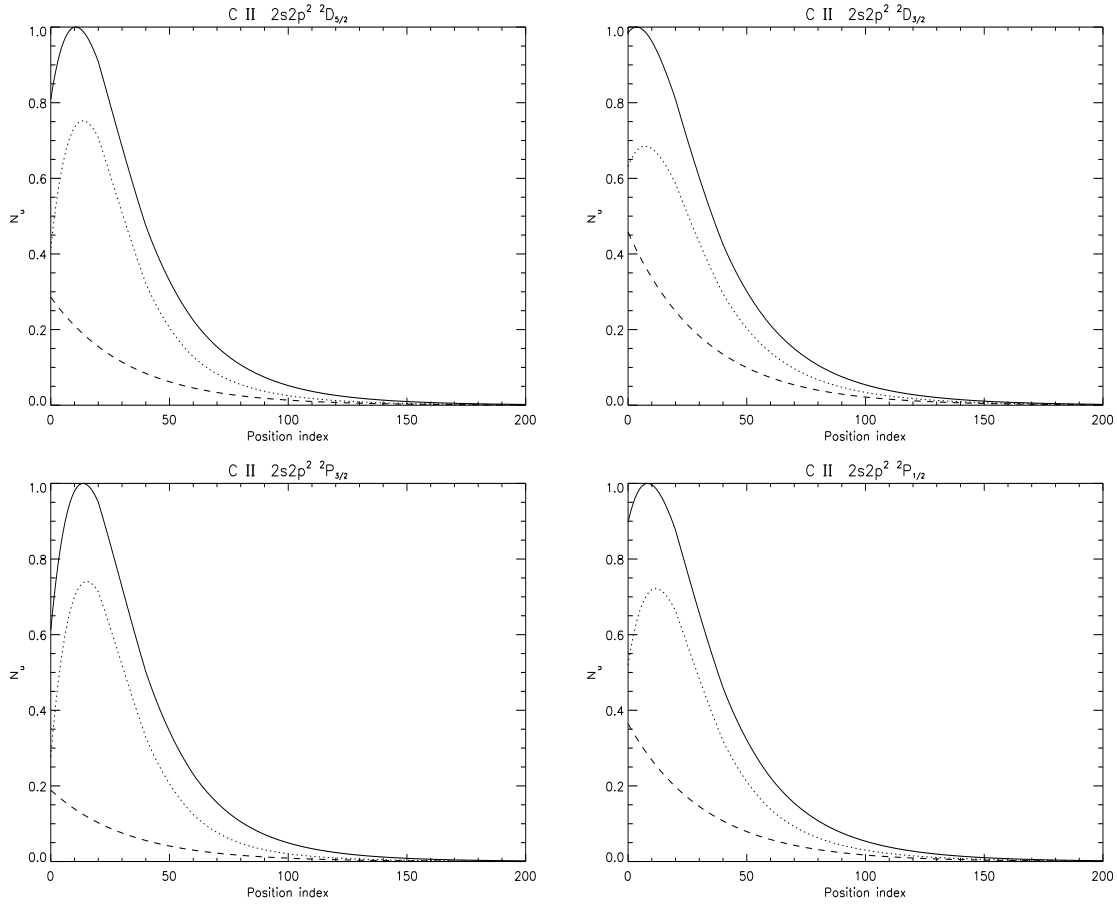

Figure A.5: Upper level population densities versus spatial position for selected lines of C II calculated in an exponential density model as in figs A.3 and A.4 but just in the most optically thick case. The solid and dotted lines are as in figs A.3 and A.4

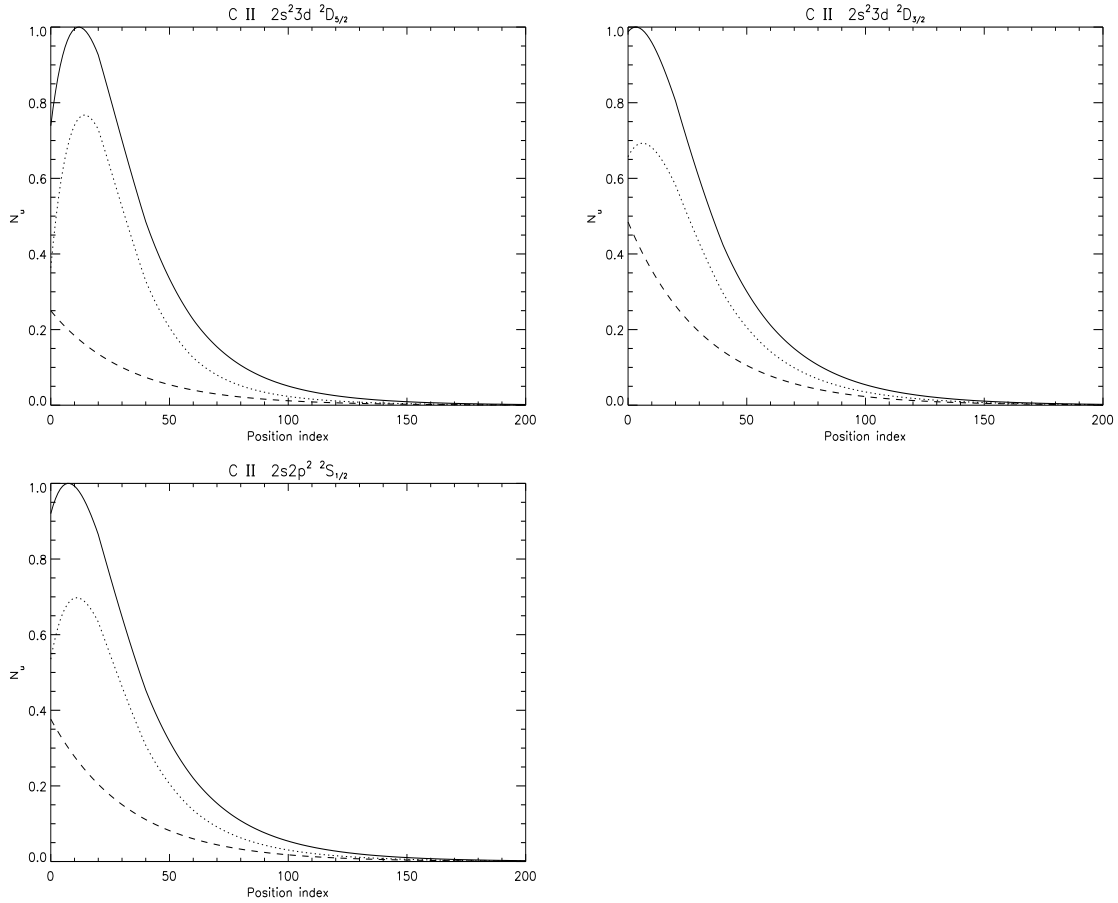

Figure A.6: Upper level population densities versus spatial position for selected lines of C II calculated in an exponential density model as in fig. A.5. These plots are comparable with those in fig. 3.11

Appendix B

The effect of line blending: results for the exponential density case

The absorption factors shown in figs 4.7 and 4.8 and the corresponding density distributions shown in figs 4.10 $\rightarrow$ 4.13 are shown here for an exponential density model (model 3). The agreement between $\Lambda^{(i)}(\tau_0, x)$ and $\mathcal{G}^{(i)}(\tau_0, x)$ is not greatest at layer centre but in between layer centre and the point of peak emission. Thereafter, however, the same conclusions follow as in chapter 4. The agreement between $\Lambda^{(i)}(\tau_0, x)$ and $\mathcal{G}^{(i)}(\tau_0, x)$ decreases toward the layer edges and with optical depth. There is a downward shift in the $\Lambda^{(i)}(\tau_0, x)$ values with respect to the $\mathcal{G}^{(i)}(\tau_0, x)$ ones in the blended lines. This is due to the dependence of $\Lambda^{(i)}(\tau_0, x)$ on opacity sensitive upper level population densities of overlapped components. This shift would be removed if $\mathcal{G}^{(i)}(\tau_0, x)$ were calculated iteratively. The $\Lambda^{(i)}(\tau_0, x)$ versus x trends deviate from those of $\mathcal{G}(\tau_0, x)$ most markedly for lines that share an upper level with a line thicker than themselves. The density distributions do not display these indirect effects and are modified in a similar manner to those in the constant density case but with the point of most significant modification begin between layer centre and the point of peak emission. The corresponding limb-brightening curves are shown in figs 4.14b and 4.15b.

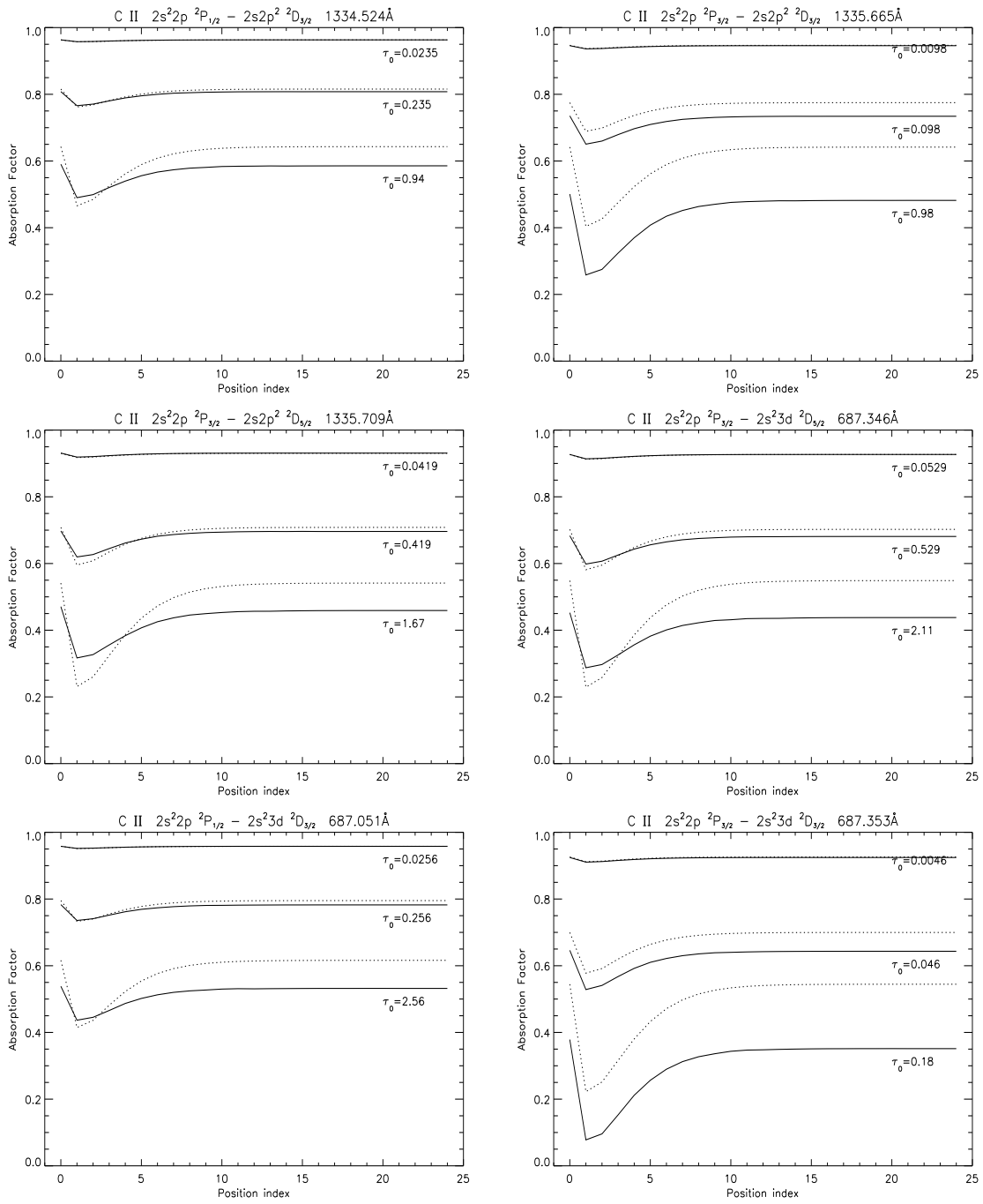

Figure B.1: Absorption factors with blending included versus position for selected lines of C II corresponding to three sets of optical depths. Absorption factors are calculated iteratively via eqs 4.18 and 2.8 in an exponential density model. The solid lines are $\Lambda^{(i)}(\tau_0, x)$ and the dotted lines are $\mathcal{G}^{(i)}\{\tau_0, x\}$. These plots are comparable with those in fig. 4.7.

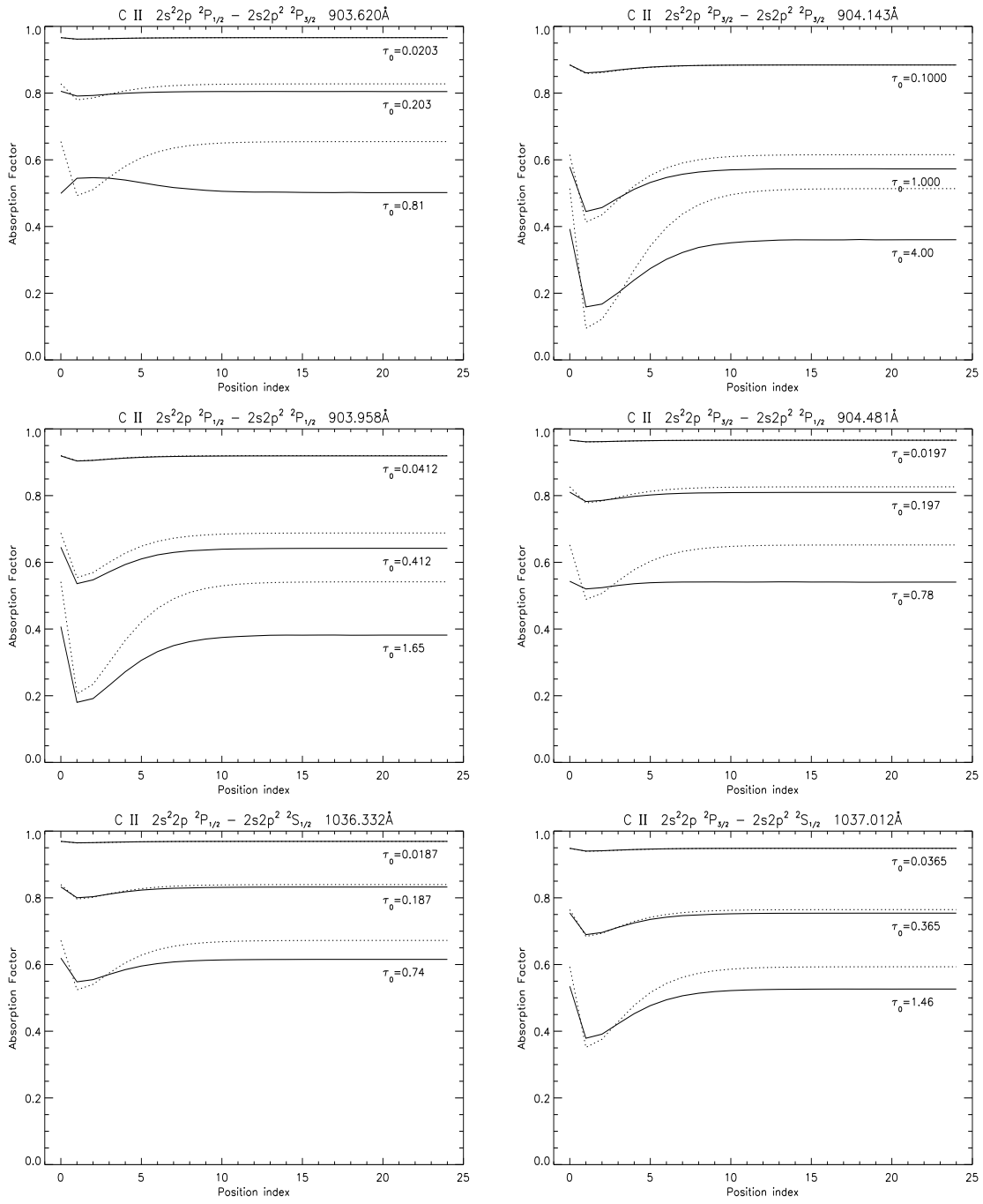

Figure B.2: Absorption factors with blending included versus position for selected lines of C II as in fig A.1. These plots are comparable with those in fig. 4.8.

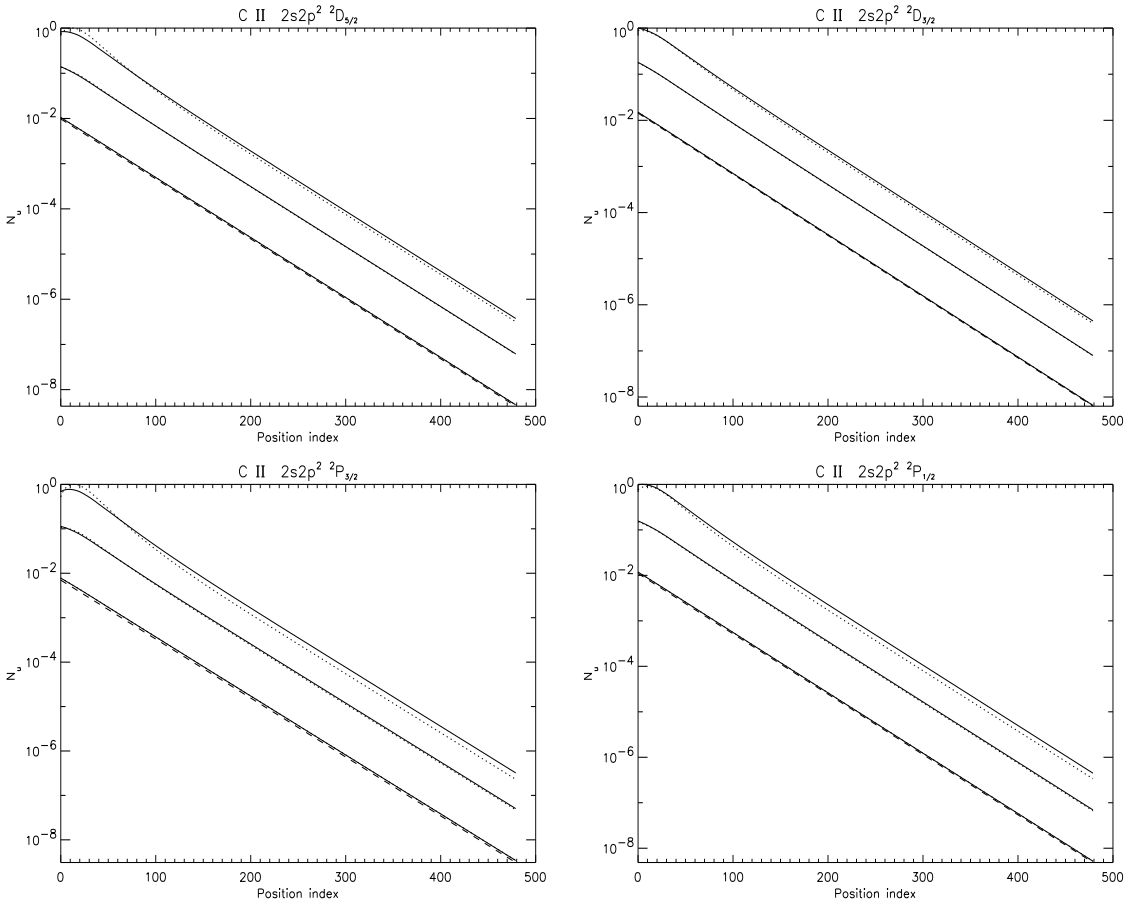

Figure B.3: Upper level population densities versus spatial position for selected lines of C II with blending effects included, calculated in an exponential density model. The solid lines correspond to calculations based on $\Lambda^{(i)}(\tau_0, x)$ for the same three sets of optical depths as in figs B.1 and B.2. The dotted lines represent the $\mathcal{G}^{(i)}(\tau_0, x)$ based calculations. These plots are comparable with those in fig. 4.10.

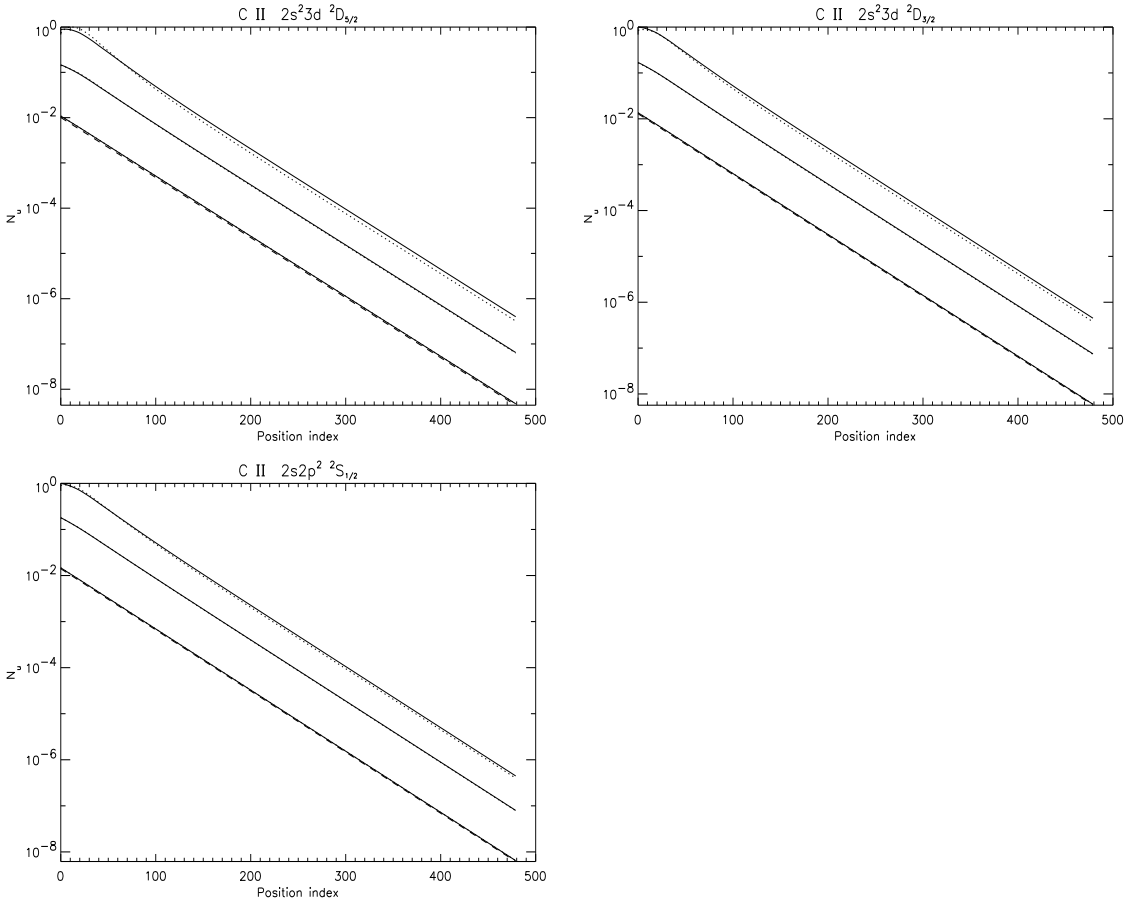

Figure B.4: Upper level population densities versus spatial position for selected lines of C II with blending effects included, calculated in an exponential density model. The solid and dotted lines are as in fig. B.3. These plots are comparable with those in fig. 4.11.

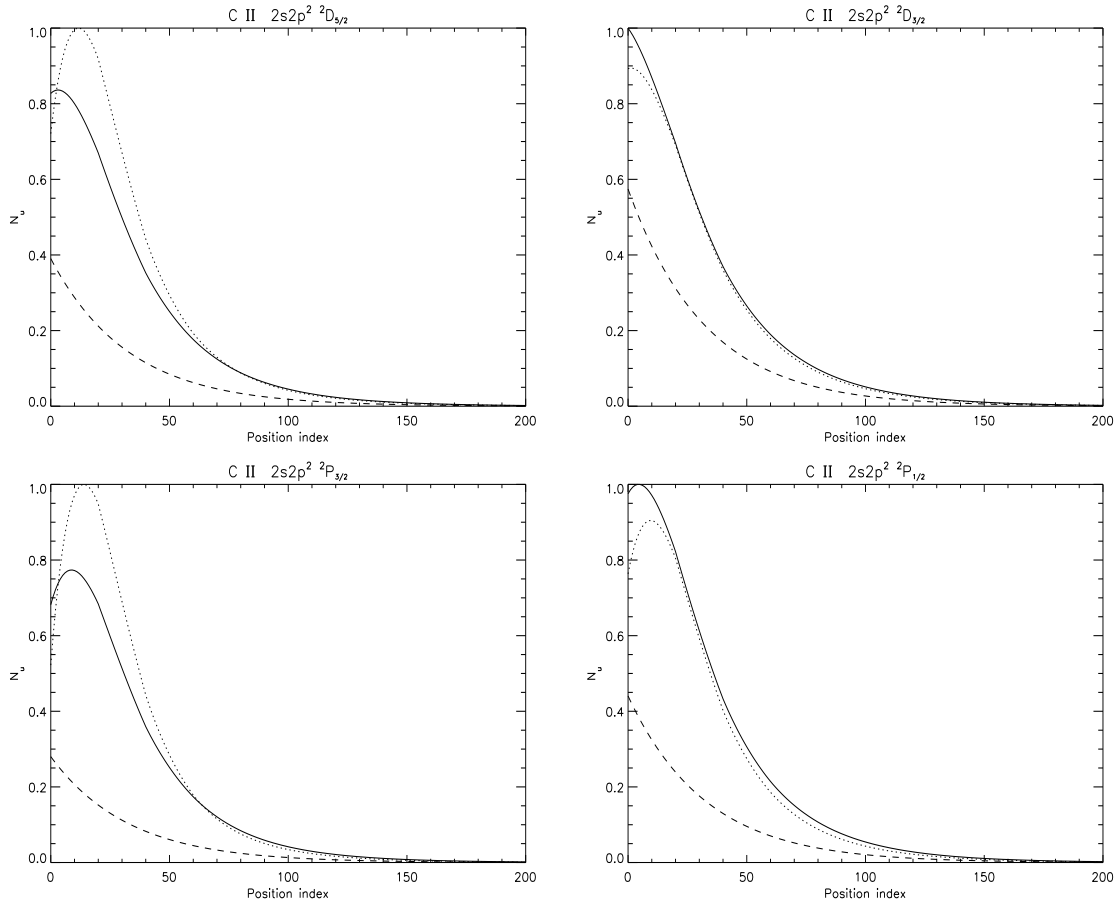

Figure B.5: Upper level population densities versus spatial position including blending effects, for selected lines of C II as in figs B.3 and B.4 but just in the most optically thick case. The solid and dotted lines are as in figs B.3 and B.4. Values are not absolute but are scaled so that the maximum population density value is unity. These plots are comparable with those in fig. 4.12.

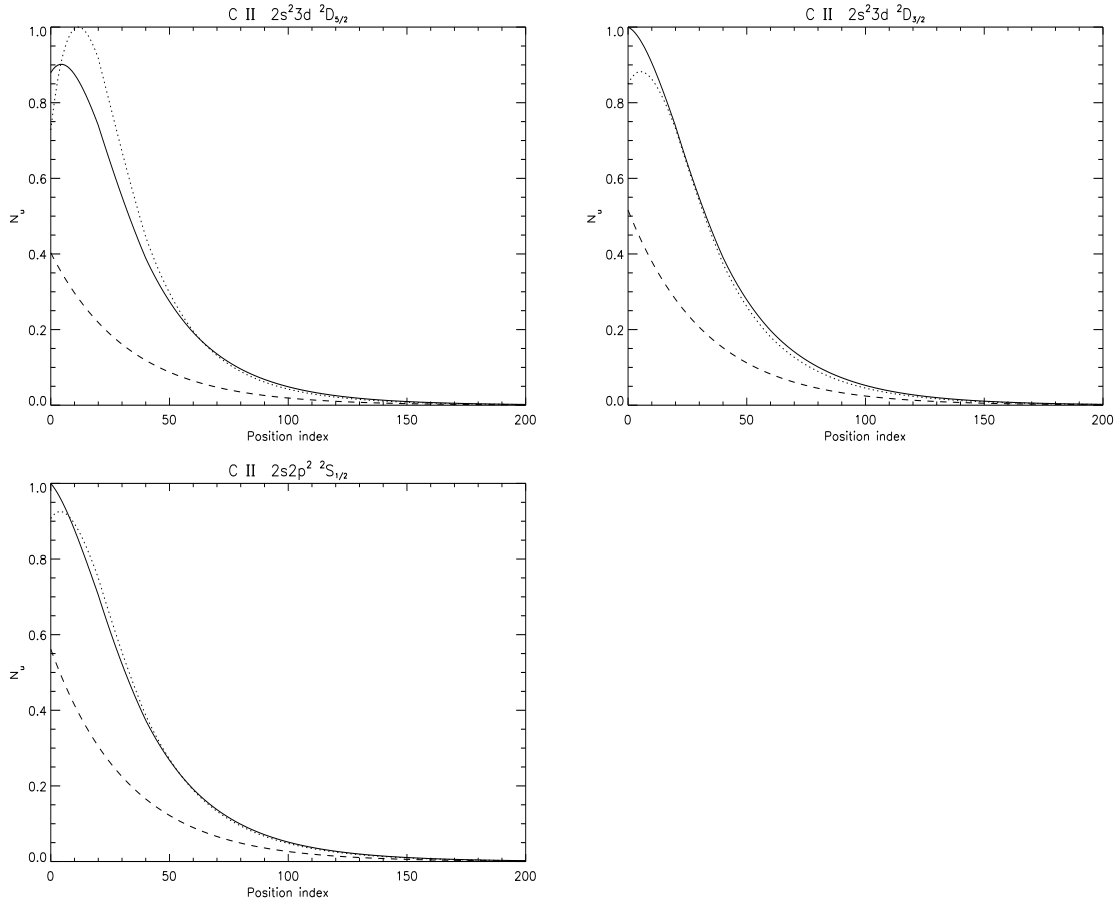

Figure B.6: Upper level population densities versus spatial position including blending effects, for selected lines of C II as in fig. B.5. Values are not absolute but are scaled so that the maximum population density value is unity. These plots are comparable with those in fig. 4.13.